Osteoarthritis and Cartilage 32 (2024) 1220–1234

Osteoarthritis and Cartilage

Review

Temporal progression of subchondral bone alterations in OA models involving induction of compromised meniscus integrity in mice and rats: A scoping review

Tamás Oláh # †, Magali Cucchiarini #, Henning Madry # *

* Center of Experimental Orthopaedics, Saarland University, Homburg, Germany
† Department of Physiology, Faculty of Medicine, University of Debrecen, Debrecen, Hungary

ARTICLE INFO

Article history:
Received 17 January 2024
Accepted 6 June 2024

Keywords:
Osteoarthritis
Subchondral bone
Meniscal injury
Mouse
Rat
Scoping review

SUMMARY

Objective: To categorize the temporal progression of subchondral bone alterations induced by compromising meniscus integrity in mouse and rat models of knee osteoarthritis (OA).
Method: Scoping review of investigations reporting subchondral bone changes with appropriate negative controls in the different mouse and rat models of OA induced by compromising meniscus integrity.
Results: The available literature provides appropriate temporal detail on subchondral changes in these models, covering the entire spectrum of OA with an emphasis on early and mid-term time points. Microstructural changes of the subarticular spongiosa are comprehensively described; those of the subchondral bone plate are not. In mouse models, global subchondral bone alterations are unidirectional, involving an advancing sclerosis of the trabecular structure over time. In rats, biphasic subchondral bone alterations begin with an osteopenic degeneration and loss of subchondral trabeculae, progressing to a late sclerosis of the entire subchondral bone. Rat models, independently from the applied technique, relatively faithfully mirror the early bone loss detected in larger animals, and the late subchondral bone sclerosis observed in human advanced OA.
Conclusion: Mice and rats allow us to study the microstructural consequences of compromising meniscus integrity at high temporal detail. Thickening of the subchondral bone plate, an early loss of thinner subarticular trabecular elements, followed by a subsequent sclerosis of the entire subchondral bone are all important and reliable hallmarks that occur in parallel with the advancing articular cartilage degeneration. Thoughtful decisions on the study design, laterality, selection of controls and volumes of interest are crucial to obtain meaningful data.

Introduction

Traumatic meniscus injury represents a key risk factor for human knee osteoarthritis (OA),[1] involving also the subchondral bone.[2–4] In late human OA with degenerated menisci in otherwise stable knees, the subchondral bone plate thickness increases.[5] In parallel, the subarticular spongiosa (trabecular bone) expands with increased BV/TV, Tb.N, Conn.Dn, BS/TV, FD and decreased Tb.Sp, Tb.Pf (Table I), reflecting sclerosis of the entire subchondral bone structure compared to normal.[5] In contrast, bone loss occurs in patients with acute meniscus tears, presenting as lower apparent trabecular BV/TV and apparent Tb.N, and greater apparent Tb.Th, and apparent Tb.Sp (Table I).[6] Due to the limited human data available, animal models are of utmost importance to further investigate these trajectories. Compromising meniscus integrity in mice and rats induces osteochondral OA changes in a defined fashion.[7,8] Their macroanatomic knee morphology is analogous to humans, even if the tibial plateau width is 26-fold smaller in mice and 11-fold smaller in rats.[9] The width ratio of both plateaus is comparable,[9] and the groove of the extensor digitorum longus tendon indenting in larger animals the anterior lateral plateau[10–12] is absent.[9] Unlike in humans, a distinct intercondylar fossa separates their tibial plateaus.[9–11]

Well-defined microstructural parameters characterize the architecture of the subchondral bone plate and the subarticular spongiosa, the two dissimilar entities comprising the subchondral bone (Table I).[13] Both undergo characteristic changes during OA,[5] and

* Correspondence to: Center of Experimental Orthopaedics, Saarland University, Kirrberger Straße, Building 37, D-66421 Homburg, Saar, Germany.
E-mail addresses: olahtamas@gmail.com (T. Oláh), mmcucchiarini@hotmail.com (M. Cucchiarini), henning.madry@uks.eu (H. Madry).

https://doi.org/10.1016/j.joca.2024.06.002

Name	Abbreviation	Definition
Bone volume fraction	**BV/TV**	Ratio of the segmented bone volume to the total volume
Specific bone surface	BS/BV	Ratio of the segmented bone surface to the segmented bone volume
Bone surface density	BS/TV	Ratio of the segmented bone surface to the total volume
Trabecular thickness	**Tb.Th**	Mean thickness of trabeculae
Trabecular separation	**Tb.Sp**	Mean distance between trabeculae
Trabecular number	**Tb.N**	Average number of trabeculae per unit length
Trabecular pattern factor	Tb.Pf	Characterizes the connectivity of the cancellous bone
Structure model index	SMI	An indicator of the structure of trabeculae (parallel plates: SMI = 0, cylindrical rods: SMI = 3)
Degree of anisotropy	DA	Indicates how highly oriented substructures are within a volume (isotropic: DA = 1, anisotropic: DA > 1)
Connectivity density	Conn.Dn	The degree of connectivity of trabeculae normalized by TV
Bone mineral density or tissue mineral density	BMD or TMD	Reflects the calcium-hydroxyapatite content of bone. TMD does not include non-bone voxels. BMD may include non-bone voxels too.

The minimum parameter set recommended for the analysis of the subchondral trabecular bone by Bouxsein et al.[41] is highlighted in bold.[55]
SMI: structure model index.
***Source*: Adapted from Bouxsein et al.[41] and Oláh et al.[55]**

Table I Osteoarthritis and Cartilage

Overview of the most frequently reported microstructural bone parameters and their definition.

considerable species-specific differences exist.[9] The subchondral bone plate in mice and rats is 4-fold thicker than in humans (normalized to the tibial plateau width). Their higher BV/TV (Table I), and lower porosity indicate a relatively thicker and more dense and compact subchondral bone plate.[9] The specific relationship of human (and larger animal) subchondral bone plate thickness to meniscus coverage, i.e. the subchondral bone plate is thinner in meniscus-covered areas than in the central areas not covered by menisci, is absent in rodents.[7] Mice and rats lack the classical osteons/Haversian systems that are composed of concentric layers of compact bone tissue surrounding a central Haversian canal, containing a blood vessel.[14] Haversian canals constitute, beside marrow spaces, the two major types of perforations in the subchondral plate in humans and larger animals[15] and may be involved in abnormal perfusion and neovascular invasion in OA.[16] The rodent subarticular spongiosa is composed of a denser, more connected network of thinner trabeculae than in humans, indicated by higher BV/TV, BS/BV, BS/TV, Tb.N, and DA, and lower Tb.Th, and Tb.Sp (Table I).[9] Because of its relatively small size, microstructural analyses in mice often comprise the entire epiphysis (excluding the growth plate), in contrast to humans. Also, their lower bone marrow adiposity[17] may affect bone metabolism and cartilage nutrition, and translate into improved biomechanical properties of the subchondral bone, similarly to younger humans,[17,18] suggesting species-specific differences in regulating local marrow niche functions and global metabolic changes.[19] The secretory active bone marrow adipose tissue contributes not only to the regulation of skeletal cell fate, homeostasis and function and whole-body energy metabolism,[19–22] but also to biomechanical properties of the subchondral bone.[18] In mice and rat menisci, ossicles develop in both horns.[23,24] Humans lack such bony nodules, although they may develop after trauma.[25,26]

Despite these differences, rodents are the most widely used OA models, and similar to humans, meniscal injuries induce subchondral bone changes. Yet, to the best of our knowledge, no study has comprehensively analyzed and categorized in a chronological and conceptual (protocol-specific) fashion the available data from studies with appropriate negative controls on alterations of the subchondral bone induced by compromising meniscus integrity to date. Such information on its temporal progression would help to select the ideal protocol, to identify optimal time points when specific changes can be expected to occur, and to serve as a basis to which future studies can compare results. This scoping review aims to gather the accessible information about subchondral bone changes in mice and rat models. It identifies new emergent perspectives, among which the importance of laterality and control selection, similarities and differences in subchondral bone changes between the diverse mouse and rat models of knee OA resulting from compromised meniscus integrity and methodical insufficiencies that may be addressed in future studies in a standardized and reproducible way.

Literature search results

The project was registered at Open Science Framework (registration number: osf.io/4fwn9; https://doi.org/10.17605/OSF.IO/4FWN9). A PubMed search was performed on 16th of January, 2024, with the terms "(osteoarthritis) AND ((meniscus) OR (meniscal) OR (meniscectomy))" yielded 5704 results, including several studies not reporting any subchondral bone data (Fig. 1). When the search was refined as "(subchondral bone) AND (osteoarthritis) AND ((meniscus) OR (meniscal) OR (meniscectomy))", it resulted in 556 papers (9.7% of the original search). In the detailed analysis, only those studies were included where OA was evoked by surgical or traumatic tear or injury of the meniscus, destabilization of the meniscus (DMM), or total or partial meniscectomy. To avoid any supplementary factors leading to additional instability such as anterior cruciate ligament transection, such combined methods were excluded (Fig. 1). Papers were also excluded if they were reviews, not in English language, full text was unavailable, did not report subchondral bone, did not report adequate controls, or OA was not induced by compromising meniscus integrity. Thus, the above selection of papers was further refined via reading their abstracts to n = 240, and after reading their full text, to a number of n = 165 papers (only 2.9% of all papers reporting meniscus-related OA), from which n = 134 mouse/rat papers were eligible for a detailed evaluation. n = 9 papers reported human, n = 23 other animal studies, including 1 paper that reported both (Fig. 1). Although a meta-analysis was originally envisioned, a scoping review was determined most appropriate because of the considerable inter-manufacturer error with different micro-CT devices[27,28] and the error range between different analyzing programs.[29,30] Since scanner and study protocol parameters (resolution, evaluation algorithm, volume of interest [VOI]) highly affect the resulting numerical values,[27–30] their in- or decreases were reported qualitatively.

Evaluation of the abundance of studies

The first study fulfilling the inclusion criteria was performed in mice, published in 2007.[31] The number of eligible papers remained

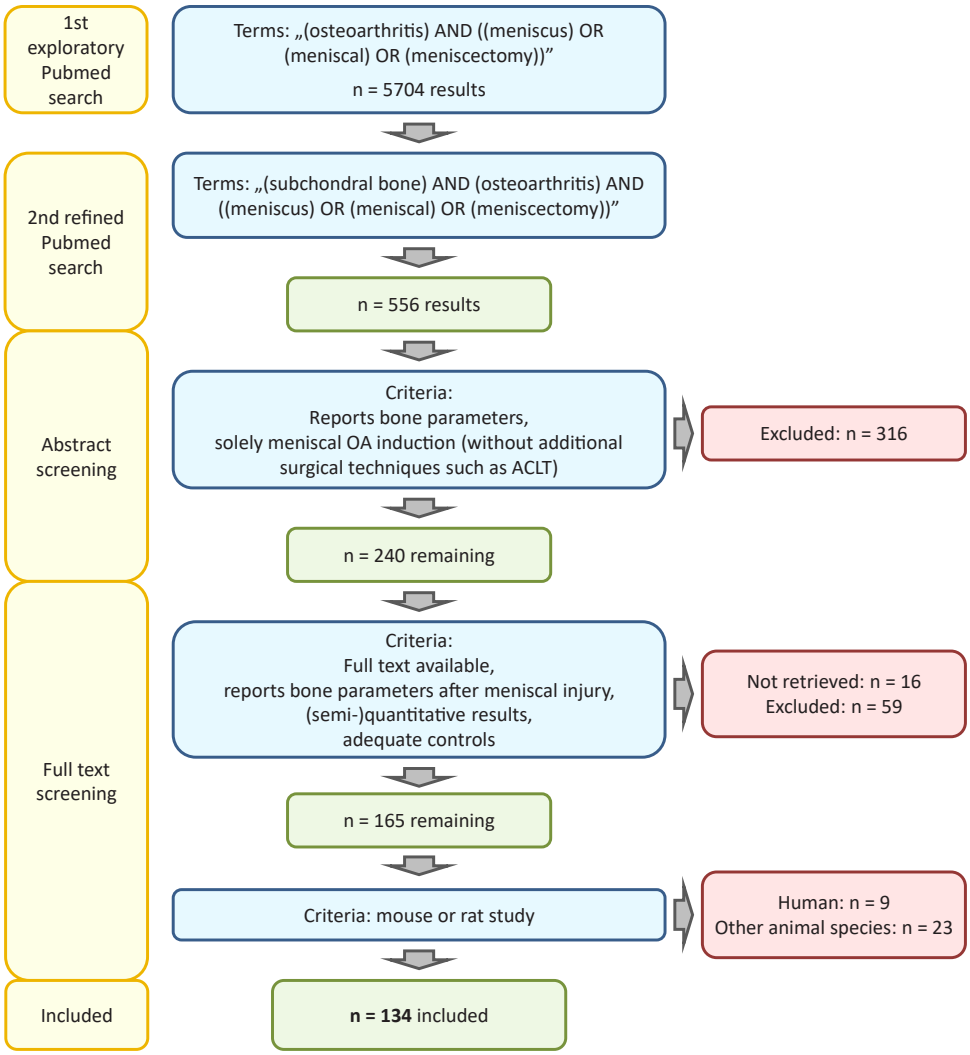

Fig. 1 Osteoarthritis and Cartilage

Flowchart of the systematic literature search resulting in n = 134 eligible papers, evaluated in the study.

relatively low thereafter (n = 1–4 per year) (Fig. 2A). After 2015, the frequency of studies rapidly increased.

Evaluation of the study designs

In the finally selected 134 papers, four main types of induced meniscal damage were described: (1) total and (2) partial meniscectomy, (3) meniscal transection or tear (MMT; the pars intermedia ["mid-body"] of the medial meniscus is transected at its narrowest point without removing parts of the meniscus, resulting in a complete radial tear, together with the medial collateral ligament [MCL]), and (4) DMM by meniscal release (nearly always the medial meniscus anterior root is transected, no parts of the meniscus are removed).

Evaluation of study methods

Micro-computed tomography (micro-CT) was used in 76.9% of all studies (n = 103; rats, mice combined) (Fig. 2B). When the occurrence of applying a combined evaluation protocol including micro-CT paired with histology, biochemistry, or gross pathology of the joint was examined, micro-CT was used alone in 51.5% of the total n = 134 studies, and in combination with histology in 20.1%. Histological evaluation was mostly applied for reporting subchondral bone plate thickness, sometimes also for evaluation of trabecular microstructure. Many of those studies did not find significant differences between groups.[32] Generally, the most frequently reported bone parameters were BV/TV, Tb.Th, Tb.Sp, Tb.N, bone mineral density (BMD), the presence of osteophytes, and subchondral bone plate thickness (Fig. 2C). The included small animal studies covered the entire time scale of OA development, with a greater emphasis at early and mid-term time points (Fig. 2D).

Mouse models of subchondral bone changes following meniscus injury

The mouse is by far the most frequently used species for studying OA caused by compromising meniscus integrity. In mice, DMM according to the classical protocol[31] was applied in the vast majority of studies (n = 102 studies), always performed as transection of the

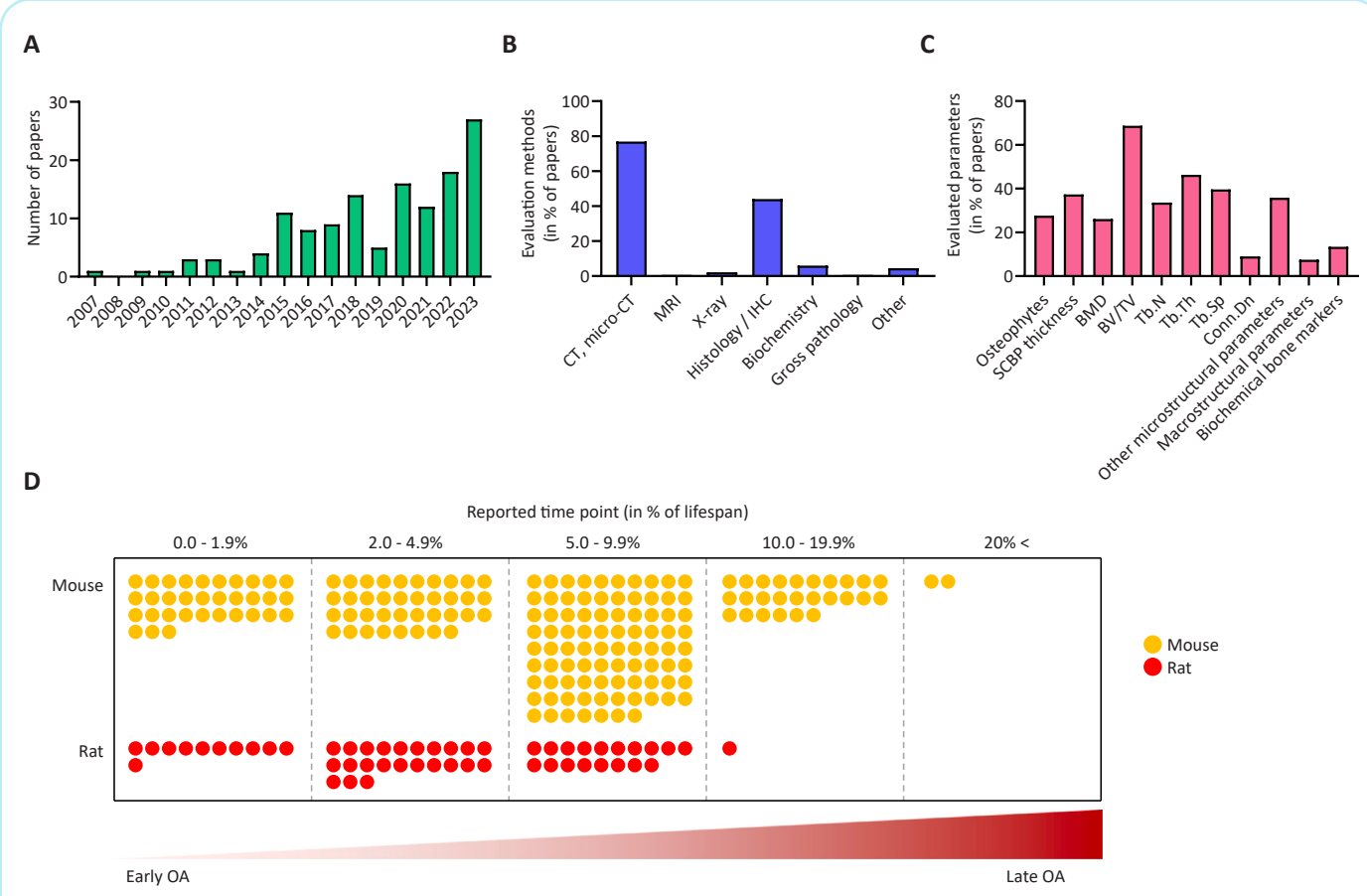

Fig. 2

Osteoarthritis and Cartilage

Summary of the n = 134 papers evaluating the subchondral bone in mouse and rat models of OA, induced by meniscus injuries. **(A)** Histogram showing the number of eligible papers per year. The most important subchondral bone **(B)** evaluation methods and **(C)** parameters most frequently reported in the studies. Of note, the cumulative percentages within the graphs may not be equal to 100% due to some studies reporting multiple techniques or parameters. **(D)** Reported time points, expressed as percentage of the average life span of the species. Dots indicate study termination time points falling into the displayed percent range. Papers reporting multiple time points are presented with multiple dots on the figure. Abbreviations: CT, computed tomography; IHC, immunohistochemistry; MRI, magnetic resonance imaging; OA, osteoarthritis; SCBP, subchondral bone plate.

medial meniscus anterior root (also termed "release of the medial meniscotibial ligament") (Supplementary Table 1). In n = 1 study, DMM was performed as a medial meniscus posterior root tear, with identical results to the conventional (anterior) DMM.[33] Total[34] or partial medial meniscectomy,[32] MMT,[35] and DMM combined with "hemisectomy" (possibly removal of half of its anterior body; no detailed protocol provided[36]) were used only in 1 study, respectively (Supplementary Table 1).

Subchondral bone changes after total and partial medial meniscectomy and MMT in mice

After total medial meniscectomy at 8 weeks, subchondral bone plate thickness increased,[34] and trabecular Tb.Th,[34] BV/TV,[34] and Conn.Dn[34] were unchanged. Partial medial meniscectomy induced no change in histological BV/TV[32] at 6 weeks. After MMT (combined with MCL tear [MCLT]) at 5 weeks, decreased BV/TV,[35] Tb.Th,[35] Tb.N,[35] BMD,[35] and increased Tb.Sp[35] were reported, indicating loss of trabecular bone. When DMM was combined with meniscus hemisectomy, subchondral bone plate thickness increased at the medial posterior femoral subregion at 14 weeks.[36]

Subchondral bone changes after DMM in mice

Between 2–12 weeks, cartilage degeneration and synovitis scores progressively worsened.[37] The time-course of the most relevant alterations of the subchondral bone plate, subarticular spongiosa, and other parameters are summarized in Tables II and III and Supplementary Table 2. DMM induces an immediate early (already after 2 h) increase in the subchondral bone plate volume (Table II). It is followed by an uncertain increase of its thickness at 0.5–2 weeks that becomes unambiguous at 4 weeks, remaining elevated until 10 months postoperatively (longest time point evaluated). Its calcium-hydroxyapatite content (reflected in bone volume or tissue mineral density) remains either unchanged or increases over time. In the subarticular spongiosa, the increase of BV/TV, starting at week 1, is an important hallmark (Table II). Although confirmed in most of the studies, no change or a decrease was also sometimes reported. At 8 weeks, most studies reporting increased BV/TV used a sham-

Time (weeks)	BV	BV/TV	Thickness	BMD or TMD	Pores, perforations	Number of cracks	Number of lacunae
Mouse DMM							
0 (2 h)	↑[63]		≈[64]				
0.5 (2-3 days)			↑,[54] ≈[65]				
1	≈[66]		≈,[64–68] ↑[54,69]	≈[66]			
2	≈[66]		≈,[65,66,70,71] ↑[64,69,72]	↑,[63] ≈[66]			
4	↑[66]		↑[64–67,69–77]	≈[66]	↑[78]	↑[79]	↓[79]
6			↑,[70,80,81] ≈[44]	↑[80]			
7			↑[82]				
8	↑[66]	↑[83]	↑,[63–67,69,71,73–77,81,84–96] ≈[36,94,95,97–101]	≈[83]			
9			↑[102]				
10			≈[44]	↑[103]			
12	↑[66]		↑,[66,88,90,93] ↓,[104] ≈[65]				
13 (3 months)			↑[105]				
20	↑[66]		↑[66]	≈[66]			
42 (10 months)			↑[36]				
Rat MMT							
1	≈[106]		≈[106]	≈[106]	≈[106]		
2				≈[107]			
3	↑[106]		↑[106]	↑[106]			
4				≈[107]	≈[108]		
6			≈[109]				
8			↑[107] ≈[110]	↓[107]			
10			↑[111,112]				
12			↑[107]	↓[107]			
Rat DMM							
1			≈[113]				↑[113]
2					↑[114]		↑[113]
4			↑[113,115]		↑[114]		↑[113]
8			↑[115,116]		↑[116]		↑[115,116]

Legends: ≈ unchanged vs. control; ↑ increased vs. control; ↓ decreased vs. control. Abbreviations: BMD, bone mineral density; BV, bone volume; BV/TV, percent bone volume; DMM, destabilization of the medial meniscus; MMT, medial meniscal transection; TMD, tissue mineral density.

Table II

Osteoarthritis and Cartilage

Time-course of change of subchondral bone plate parameters in mice and rats after DMM and MMT.

operated control group in a unilateral study design (n = 14; DMM-operated limbs compared to sham-operated limbs of different animals) (Fig. 3A, Supplementary Table S3). In contrast, studies reporting unchanged BV/TV applied a bilateral study design as dominant protocol, where the DMM-treated knee was compared to the contralateral one (sham or unoperated; n = 10) (Fig. 3B, Supplementary Table S3). In these bilateral models, animals may shift their bodyweight to the uninjured contralateral knee, possibly increasing "control" BV/TV by resulting new bone formation, masking the difference vs. the increased BV/TV of the ipsilateral OA knee, although the number of studies reporting decreased BV/TV was too low for definite conclusions (Supplementary Fig. 2). The subarticular trabecular structure becomes more disconnected with more rods, beginning at 2–4 weeks, as indicated in mostly increased Tb.Pf, and structure model index (SMI), and decreased Conn.Dn and trabecular bone area. These alterations persisted at the later stages too. Other parameters, such as BV, BMD, Tb.Th, and Tb.Sp did not show consistent changes, they increased, decreased or did not change within or across time points and studies. Of note, osteophytes do not develop before 1 week (Supplementary Table 2). Generally, the subchondral bone plate is mainly characterized by sclerosis (localized bone formation, resulting in increased bone mass) based on the published literature. Major alterations in the subarticular spongiosa are the increased bone volume with a structurally degenerative and less connected phenotype (Fig. 4A and D, Supplementary Fig. 1).

Rat subchondral bone changes following meniscus injury

In rats, OA induction termed "medial meniscal tear" (MMT; also referred to as medial meniscal transection) by transecting the medial meniscus thus inducing a complete radial tear (functionally similar to a total meniscectomy) combined with an MCLT was the most common method (n = 17 studies investigating 8 different time points) (Supplementary Table 4). DMM by transecting the meniscus (anterior) root (without MCL) was performed in n = 10 studies. Partial (anterior) medial meniscectomy was applied in n = 2 studies (Supplementary Table 4).

Subchondral bone changes in rat MMT models

Subchondral bone plate thickness increased at 3 weeks, persisting to later stages (Table II). Importantly, MMT has a biphasic effect on the subarticular spongiosa (Table III). In early OA, both BV/TV and Tb.Th decrease, and Tb.Sp increases. A shift of the direction of these three parameters occurs around 6–8 weeks. Thereafter, BV/TV and Tb.Th increase, and Tb.Sp decreases. BMD, Tb.N, and Conn.Dn remained low at all examined time points. Osteophytes were detected continuously, beginning to occur at 3 weeks (Supplementary Table 2). Thus, MMT results not only in a thicker subchondral bone plate, but also in a degenerative subchondral trabecular bone

Time (weeks)	BV/TV med:lat ratio	BV/TV	BV	BMD or TMD	Tb.Th	Tb.Sp	Tb.N	Tb.Pf	SMI	Conn.Dn	TV	BS	BS/BV	DA	Trab. bone area
Mouse DMM															
0						≈[64]									
0.5 (2-3 days)	≈[72]														
1	≈[72]	↑[54,69]	≈[66]	≈[66]		≈[64]									
2		↑[69,72,117,118] ≈[70]	≈[66]	≈[66]		↑[119,120] ↓[64]		↑[71] ≈[70]	↑[71]						
4		↑[66,69,70,72,78,79,118,121,122] ≈[74,123–125] ↓[87,126,127]	↓[66]	↓[124,127] ≈[66,125] ↑[85]	↑[78,79,121,122,125,128] ↓[126,129,130] ≈[123]	↓[64,121,122] ↑[126,127] ≈[79,125]	↓[122,125,126,130] ≈[79,131]	↑[70,71]	↑[71,130]	↓[126]	↓[121]	↓[129]	≈[131]		↓[77]
5				↓[117]											
6		↑[45,70,80] ≈[123,132,133]	↑[45]	≈[80,133]	≈[80,133,134] ↑[123]	↓[80,134]		↑[70]							
8		↑[33,69,74,75,93,95,96,126,127,135–142] ≈[37,83,84,96,97,99–101,124,125,143–147] ↓[42,43,87,148]	↓[42,43,66] ↑[90]	↑[75,85,90,125,127,141,142] ≈[66,83,96,124,143,149] ↓[37]	≈[37,83,84,96,97,99–101,129,130,143–145,150] ↑[75,96,125,126,128,135–141,151] ↓[42–44,87,95,148]	≈[37,84,96,97,101,125,140,143–145,148] ↓[64,119,120,126,127,135,136,138,139,142,151] ↑[42–44,137,150]	≈[37,96,97,99,101,131,138,144,145] ↓[42–44,125,126,130,137,148,150] ↑[95,100,140,151]	≈[97] ↑[71]	≈[84,96,144] ↑[71,130]	↓[96,126] ≈[84]			↑[37,148] ≈[83,131]		↓[77]
9		≈[102]			↑[102]		≈[102]								
10				↑[152] ↓[117]	↑[134]	≈[134]									
12		≈[124,138,145,153] ↑[88,93] ↓[104]	↑[90] ↓[66]	≈[66,124] ↑[90]	↑[88,153,154] ≈[130,138,145]	≈[88,138,145,153] ↑[104]	↓[104,130,153] ≈[138,145]		↑[130,153]	↓[153]			↓[153]	↑[153]	
16		≈[155]													
17 (4 months)					≈[156]		≈[156]								
19					≈[133]										
20			↓[66]	≈[66]											
42 (10 months)		≈[36]			≈[36]		↓[36]		≈[36]						
Rat MMT															
2		↓[107,157]		≈[107]	↓[107,157]	↑[107,157]	↓[107,157]			↓[107,157]					
3		↓[158,159]		↓[158]	↓[158]	↑[158,159]	↓[158]								
4		↓[107,157]		≈[107]	↓[107,157]	↑[107,157]	↓[107,157]			↓[107,157]					↑[160]
6		↓[158]		↓[158]	↑[158,159]	↑[158]	↓[158]			↓[158]					↑[160]
8		↑[107,157] ↓[161]		↓[107]	↑[107,157]	↓[107,157]	↓[157]			↓[157]					
12		↑[107,157]		↓[107]	↑[107,157] ≈[162]	↓[107,157] ≈[162]	↓[157] ≈[162]			↓[157]			≈[162]		
Rat DMM															
1		≈[113]													
2		↓[163]			↓[163]	↑[163]	≈[163]			↓[163]					
4		↓[113,163,164]			↓[163,164]	↑[163,164]	↓[163,164]			↓[163,164]					
8		↑[163,164] ↓[116]			↑[163–165] ≈[116]	≈[116,163–165]	↓[163,164] ≈[165]			↓[163,164]					
12		↑[163]			↑[163]	≈[163]	↓[163]			↓[163]					

Legends: ≈ unchanged vs. control; ↑ increased vs. control; ↓ decreased vs. control. Abbreviations: BMD, bone mineral density; BV, bone volume; BV/TV, percent bone volume; DMM, destabilization of the medial meniscus; MMT, medial meniscal transection; SMI: structure model index; TMD, tissue mineral density.

Table III

Time-course of change of subchondral trabecular bone parameters in mice and rats after DMM and MMT.

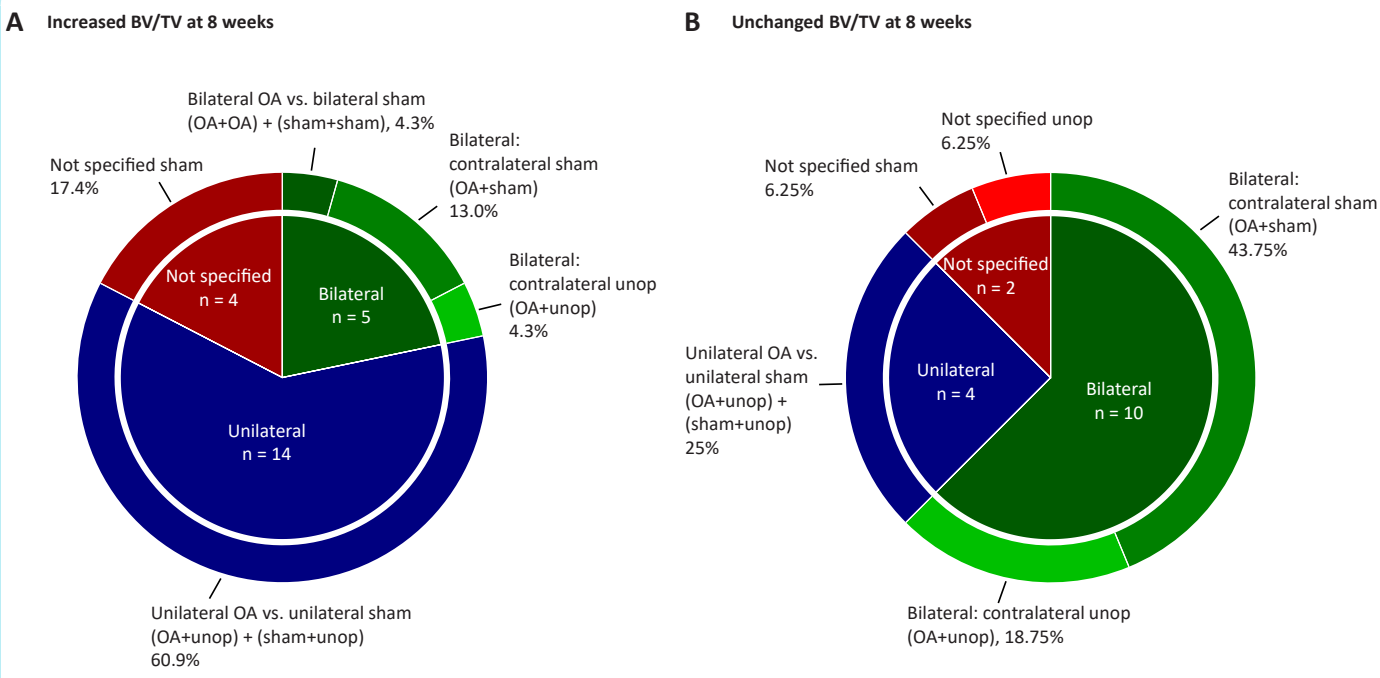

Fig. 3 Osteoarthritis and Cartilage

Heterogeneity of the study designs and control groups. Pie diagrams show the numbers and percentages of studies applying bilateral or unilateral study designs for reporting BV/TV data following DMM in mice, at the 8-week time point. Possible study designs and control groups were the following: (1) bilateral OA (left OA+ right OA knee) vs. bilateral sham (sham+sham); (2) bilateral with contralateral sham (OA+sham); (3) bilateral with contralateral unoperated (OA+unop); (4) unilateral OA (OA+unop) vs. unilateral sham (sham+unop); (5) unilateral OA (OA+unop) vs. unilateral unop (unop+unop); (6) not specified sham; (7) not specified unop. **(A)** Distribution of studies that reported increased BV/TV. **(B)** Distribution of studies that reported unchanged BV/TV. Abbreviations: BV/TV, bone volume fraction; DMM, destabilization of the medial meniscus; unop, unoperated.

phenotype with decreased bone mass, connectivity, and mineralization. These earlier changes probably result from the loss and thinning of trabeculae, while later stages manifest in a sclerotic phenotype with increased bone mass, thicker trabeculae, and a loss or fusion of smaller trabeculae, but still low connectivity and mineralization.

Subchondral bone changes in rat DMM models

Tables II and III and Supplementary Table 2 summarize the time-course of the most relevant structural alterations of the subchondral bone plate, the subarticular spongiosa (Table III) and osteophytes and other parameters (Supplementary Table 2).

DMM has a biphasic effect on the rat subchondral bone, similar to MMT (with a shift at 8 weeks). Subchondral bone plate porosity and thickness start to increase at 1–2 and 4 weeks, respectively, continuously persisting until late stages of OA (Table II). In the subarticular spongiosa, early OA manifested in a decreased BV/TV and Tb.Th, and an increased Tb.Sp as early as 2 weeks (Table III). These indicate a clear loss of trabecular bone volume, similar to the corresponding time points of MMT models. In later stages, BV/TV and Tb.Th increase, Tb.Sp remains unchanged. Osteophytes were present (Supplementary Table 2), subchondral trabecular Tb.N and Conn.Dn decrease. Altogether, these changes point towards a thickening of the trabeculae with a loss or fusion of smaller trabeculae, similarly as in advanced OA following MMT.

Subchondral bone changes in rat models of partial medial meniscectomy

Partial medial meniscectomy did not change subchondral bone plate thickness at 8 weeks.[38] At 16 weeks (partial meniscectomy plus MCLT), decreased BV,[39] BV/TV[39] and Tb.N,[39] unchanged Tb.Th[39] and Tb.Sp,[39] and increased osteophyte formation[39] were reported.

In sum, the rat is popular and widely used for studying the structural consequences of compromising meniscus integrity. MMT and DMM resulted in highly similar subchondral bone OA phenotypes (Supplementary Table 4, Fig. 4B and C), even though in MMT, the MCL is transected in addition to the severe meniscus injury. Both MMT and DMM models induce a specific biphasic temporal pattern of subchondral bone changes in parallel with advancing cartilage damage, involving decreasing biomechanical properties and progressive osteophyte development (Supplementary Table 4, Fig. 4B and C). The thickening of the subchondral bone plate begins at week 3 or 4. At time-points of 2–6 weeks, most studies revealed early bone resorption with reduced subarticular trabecular bone volume, thickness, number, connectivity, and mineralization (Supplementary Table 4, Fig. 4B and C, Supplementary Fig. 1). The reversal point for the trabecular bone is around 8 weeks, shifting from bone loss to bone accretion. At a mid-term or late OA time point (8–12 weeks), bone accretion occurs with increased subchondral bone plate thickness, subchondral trabecular bone volume and thickness, but still low trabecular number, connectivity, and mineralization, and poor biomechanical properties (Supplementary Table 4, Fig. 4B and C, Supplementary Fig. 1). Although generally in line with those

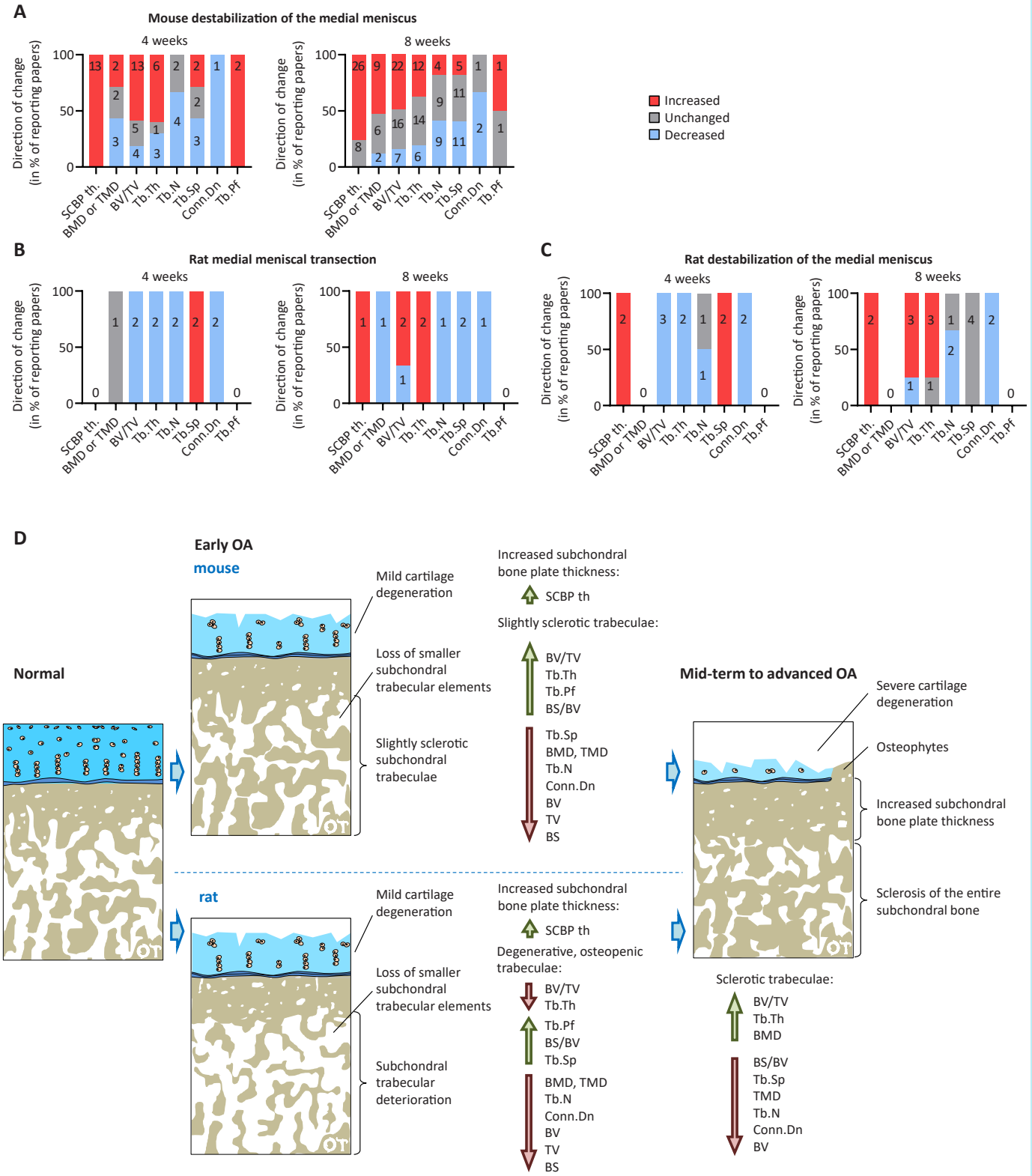

(caption on next page)

Fig. 4

Osteoarthritis and Cartilage

Subchondral bone changes in OA after meniscal injuries. **(A-C)** Numbers and ratios of studies reporting the directions of changes of the individual bone microstructural parameters at the different stages of OA. Stacked column diagrams showing **(A)** mouse DMM, **(B)** rat medial meniscal transection, and **(C)** rat DMM-induced early and mid-term OA-evoked changes of the bone microstructural parameters. Numbers in columns show the number of studies evaluated. **(D)** Schematic figure of OA subchondral bone changes in rodents. In mice, in early OA, parallel with mild cartilage degeneration, the trabecular bone becomes slightly sclerotic, with loss of smaller trabecular elements. In rats, in early OA, an overall deterioration of the trabecular bone is observed, with loss of smaller trabecular elements and decreased bone volume, mineralization, and structural complexity. In mid-term to advanced OA, the erosion of the cartilage worsens, and an overall sclerosis of the entire subchondral bone can be observed with osteophytes, increased subchondral bone plate thickness, trabecular mineralization, volume, and thickness and reduced marrow spaces. Abbreviations: BMD, bone mineral density; BS, bone surface; BS/BV, bone surface-to-volume ratio; BS/TV, bone surface density; BV, bone volume; BV/TV, percent bone volume; Conn.Dn, connectivity density; OA, osteoarthritis; SCBP th., subchondral bone plate thickness; Tb.N, trabecular number; Tb.Pf, trabecular pattern factor; Tb.Sp, trabecular separation; Tb.Th, trabecular thickness; TMD, tissue mineral density; TV, tissue volume.

observed at the later time points in mice, the findings in rats are more consistent. This may be partly due to the more homogenous study designs and the reduced number of investigations. Taken together, rat models, independently from the applied surgical technique, relatively faithfully mirror the early bone loss detected in other animal model species, and the late subchondral bone sclerosis observed in human advanced OA.

Discussion

The available literature provides appropriate temporal detail on subchondral changes in mice and rat models after meniscus injury, covering the entire spectrum of OA with an emphasis on early and mid-term time points. In mouse models, global subchondral bone alterations are unidirectional, involving an advancing sclerosis of the trabecular structure over time. Reported changes in mice (DMM) are less consistent compared to rats. In rats, subchondral bone alterations are biphasic (although supported by fewer studies). They begin with an early osteopenic degeneration and loss of the subchondral trabeculae, then progressing to a late sclerosis of the entire subchondral bone. Rat models, independently from the applied technique, therefore relatively faithfully mirror the early bone loss detected in larger animal model species, and the late subchondral bone sclerosis observed in human advanced OA. Microstructural changes of the subarticular spongiosa are comprehensively described; those of the subchondral bone plate are not. The most frequently reported parameters were BV/TV, Tb.Th, and Tb.Sp of the subarticular spongiosa and subchondral bone plate thickness. Study design, laterality, and selection of controls, all possibly affecting load bearing and consecutive bone remodeling, may considerably impact study outcomes, especially in mouse models.

Mice and rat models comprise the majority of all studies reporting subchondral changes after compromising meniscus integrity. These frequently covered a broad time scale and multiple end points. Only a low percentage of the identified studies report subchondral bone characteristics, although their number considerably increased recently. Mice are more frequently used than rats, OA has been induced solely in the medial tibiofemoral compartment, mostly by DMM, in the right knee, in a unilateral study design. Micro-CT, the gold standard for evaluating bone microstructure,[40] was chiefly applied. Histological evaluation was also performed, mainly to evaluate subchondral bone plate thickness and sometimes subchondral trabecular microstructure, despite the limitations of 2D analyses.[41]

In mice, DMM induces an immediate and sustained increase of the subchondral bone plate thickness. In the subarticular spongiosa, BV/TV mostly, but inconsistently increased, BMD remained either unchanged or increased. Although BV/TV is affected by BV and TV too, BV/TV and BV (where reported together) mostly changed identically,[39,42–45] thus, TV barely influenced the results. Subarticular spongiosa Tb.Pf, and SMI mostly increased, Conn.Dn and trabecular bone area always decreased after 2–4 weeks. Other parameters changed inconsistently. In rats, at 4 weeks, DMM and MMT prompts similar changes in the subarticular spongiosa including increased Tb.Sp and decreased BV/TV, Tb.Th, and Tb.N, and Conn.Dn (Fig. 4B and C). At 8 weeks, subchondral bone plate thickness increased, and Tb.N and Conn.Dn decreased, while BV/TV was inconclusive with both methods (Fig. 4B and C).

Importantly, when DMM in mice and in rats are compared, especially at the early time points, major species-specific differences exist (Fig. 4A and C). At 4 weeks, subchondral bone plate thickness increased, and Tb.N and Conn.Dn in the subarticular spongiosa decreased in both species. At the same time, in rats, BV/TV and Tb.Th decreased, while in mice the change of these parameters was inconclusive or rather increasing (Fig. 4A and C). These findings might be due to the slightly different lifespan, joint structure[11] and velocity of OA development of the species, besides individual study designs. Shifting the body weight from the injured to the contralateral control limb may cause unequal bone remodeling. Thus, to avoid false effects, we recommend to compare bilateral OA induction (one group of animals) with bilateral sham controls (other group of animals), or to compare only groups where one group receives unilateral OA induction and the contralateral knee remains unoperated with a group receiving unilateral sham operation and the contralateral knee remains unoperated.[46]

The available data suggest that OA development in the rat subchondral bone is of a biphasic nature. First, an osteopenic degradation of the trabecular elements and loss of bone volume occurs. This is accompanied by an increase of subchondral bone plate porosity as early as 1–2 weeks, while its thickness increased, all persisting to later stages. In these stages (from 6–8 weeks), many of the above changes reversed, indicating gain of bone volume and subchondral sclerosis (Table II, Supplementary Table 1; Fig. 4). In mice, this biphasic OA pattern was less obvious, possibly due to inhomogeneous study designs and controls in these studies. Thus, a mild OA stage characterized by subarticular trabecular bone loss may be defined, and an advanced stage when bone accretion occurs. The "osteoporotic" OA phenotype[47–49] might therefore reflect an earlier stage[50] of traumatically induced OA.

In aging-related spontaneous OA, including both the STR/Ort[51,52] and the senescence-accelerated mouse (SAM)-prone 8 (SAMP8) mouse models,[53,54] subchondral bone changes preceded the development of severe articular cartilage lesions. In both strains, subchondral bone plate thickness and BV/TV increased gradually with aging.[51–54] Furthermore, in STR/Ort mice, trabecular Tb.Th, Tb.Sp, and Tb.Pf increased, and the total porosity of the entire subchondral

bone decreased between 1 to 10 months,[51,52] and in SAMP8 mice, BMD decreased vs. control.[53,54] However, in spontaneous OA models, the degree, time dependence, and location of damage is less consistent, and a direct comparison to models of meniscus injury not feasible due to dissimilar time-scales.

A detailed, quantitative 3D microstructural assessment of the subchondral bone is not (yet) a current standard practice (performed in ~2/3 of the studies), limiting our knowledge. Furthermore, often only qualitative parameters or a single value (mostly BV/TV, BMD or bone plate thickness) were reported. Only 26.1% (n = 35) of all examined studies determine all of the four trabecular parameters recommended by the guidelines for rodents[41] (BV/TV, Tb.Th, Tb.Sp, and Tb.N) (Table I), and only 1.5% (n = 2) of all studies report an extended parameter set including subchondral bone plate thickness (and information on osteophytes).[55] In the future, methodical standardization of the evaluation techniques taking advantage of the full potential of micro-CT and reported parameters may be beneficial. It could be achieved by reporting the recommended minimum micro-CT parameter set,[41] together with bone plate thickness and osteophytes[55] to be able to compare models and time-points. Moreover, delimitation of analysis VOIs would also benefit from standardization, as in the evaluated papers VOIs covered either (1) separately the subarticular spongiosa and the subchondral bone plate, (2) the entire subchondral bone including the subarticular spongiosa and bone plate together, (3) the entire knee joint including the joint space too, or (4) their location was not defined clearly. Always separating the subchondral bone plate from the subchondral trabecular bone VOIs (e.g. by using semi-automated segmentation methods[56,57]) -reflecting its anatomical structure-, and reporting the segmentation method appears to be valuable.[9] Notably, certain parameters of trabecular microstructure (Tb.N, Tb.Th, Tb.Sp, or Conn.Dn), are meaningless if determined in a combined VOI.

Limitations include the absence of a meta-analysis caused by the methodological heterogeneity of published structural parameters. Also, while nearly always OA is induced by a traumatic tear, degenerative tears are clinically more present.[58] The vast majority of the studies used males, as DMM in male rodents evokes more severe OA.[59] Pre-clinical studies should also consider sex differences.[60,61] Validation by detailed longitudinal studies reporting early, mid-term, and late bone microstructure with appropriate normal controls relating to human knee OA caused by meniscus lesions are needed to determine whether these models faithfully represent the clinical condition.[62]

Conclusions

Mice and rats allow to study the microstructural consequences of compromising meniscus integrity at high temporal detail. Thickening of the subchondral bone plate, an early loss of thinner subarticular trabecular elements, followed by a subsequent sclerosis of the entire subchondral bone are all important and reliable hallmarks that occur in parallel with the advancing articular cartilage degeneration. Thoughtful decisions on the study design, control group and volumes of interest are crucial to obtain meaningful data.

Role of the funding source

The funders had no role in the study design, collection, analysis and interpretation of data; in the writing of the manuscript; and in the decision to submit the manuscript for publication.

CRediT authorship contribution statement

HM and TO conceptualized the study; TO acquired data, collected references, and prepared the figures and tables; TO, MC, and HM wrote the initial draft. All authors contributed to editing and revising the manuscript, and have approved the submitted version of the manuscript.

Data availability statement

All relevant data are included in the manuscript and its Supporting Information.

Declaration of Competing Interest

The authors declare no conflict of interest.

Acknowledgments

Funded by the Center of Experimental Orthopaedics.

Appendix A. Supporting information

Supplementary data associated with this article can be found in the online version at doi:10.1016/j.joca.2024.06.002.

References

1. Englund M, Guermazi A, Roemer FW, Aliabadi P, Yang M, Lewis CE, *et al*. Meniscal tear in knees without surgery and the development of radiographic osteoarthritis among middle-aged and elderly persons: the Multicenter Osteoarthritis Study. Arthritis Rheum 2009;60:831–9.
2. Roelofs AJ, De Bari C. Osteoarthritis year in review 2023: Biology. Osteoarthritis Cartilage 2024;32:148–58.
3. Ghouri A, Muzumdar S, Barr AJ, Robinson E, Murdoch C, Kingsbury SR, *et al*. The relationship between meniscal pathologies, cartilage loss, joint replacement and pain in knee osteoarthritis: a systematic review. Osteoarthritis Cartilage 2022;30:1287–327.
4. Englund M, Roemer FW, Hayashi D, Crema MD, Guermazi A. Meniscus pathology, osteoarthritis and the treatment controversy. Nat Rev Rheumatol 2012;8:412–9.
5. Olah T, Reinhard J, Gao L, Haberkamp S, Goebel LKH, Cucchiarini M, *et al*. Topographic modeling of early human osteoarthritis in sheep. Sci Transl Med 2019;11, eaax6775.
6. Kumar D, Schooler J, Zuo J, McCulloch CE, Nardo L, Link TM, *et al*. Trabecular bone structure and spatial differences in articular cartilage MR relaxation times in individuals with posterior horn medial meniscal tears. Osteoarthritis Cartilage 2013;21:86–93.
7. Zaki S, Blaker CL, Little CB. OA foundations – experimental models of osteoarthritis. Osteoarthritis Cartilage 2022;30:357–80.
8. Little CB, Hunter DJ. Post-traumatic osteoarthritis: from mouse models to clinical trials. Nat Rev Rheumatol 2013;9:485–97.
9. Michaelis JC, Olah T, Schrenker S, Cucchiarini M, Madry H. A high-resolution cross-species comparative analysis of the subchondral bone provides insight into critical topographical patterns of the osteochondral unit. Clin Transl Med 2022;12, e745.
10. Olah T, Cai X, Michaelis JC, Madry H. Comparative anatomy and morphology of the knee in translational models for articular cartilage disorders. Part I: large animals. Ann Anat 2021;235, 151680.
11. Olah T, Michaelis JC, Cai X, Cucchiarini M, Madry H. Comparative anatomy and morphology of the knee in translational models for articular cartilage disorders. Part II: small animals. Ann Anat 2021;234, 151630.
12. Olah T, Reinhard J, Gao L, Goebel LKH, Madry H. Reliable landmarks for precise topographical analyses of pathological structural changes of the ovine tibial plateau in 2-D and 3-D subspaces. Sci Rep 2018;8:75.

13. Madry H, van Dijk CN, Mueller-Gerbl M. The basic science of the subchondral bone. Knee Surg Sports Traumatol Arthrosc 2010;18:419–33.
14. Jilka RL. The relevance of mouse models for investigating age-related bone loss in humans. J Gerontol A Biol Sci Med Sci 2013;68:1209–17.
15. Clark JM. The structure of vascular channels in the subchondral plate. J Anat 1990;171:105–15.
16. Ching K, Houard X, Berenbaum F, Wen C. Hypertension meets osteoarthritis – revisiting the vascular aetiology hypothesis. Nat Rev Rheumatol 2021;17:533–49.
17. Li Z, MacDougald OA. Preclinical models for investigating how bone marrow adipocytes influence bone and hematopoietic cellularity. Best Pract Res Clin Endocrinol Metab 2021;35, 101547.
18. Simkin PA. Marrow fat may distribute the energy of impact loading throughout subchondral bone. Rheumatology 2018;57:414–8.
19. Li Z, Hardij J, Bagchi DP, Scheller EL, MacDougald OA. Development, regulation, metabolism and function of bone marrow adipose tissues. Bone 2018;110:134–40.
20. Tencerova M, Ferencakova M, Kassem M. Bone marrow adipose tissue: role in bone remodeling and energy metabolism. Best Pract Res Clin Endocrinol Metab 2021;35, 101545.
21. Kawai M, Devlin MJ, Rosen CJ. Fat targets for skeletal health. Nat Rev Rheumatol 2009;5:365–72.
22. Stegen S, Carmeliet G. Metabolic regulation of skeletal cell fate and function. Nat Rev Endocrinol 2024. Online ahead of print.
23. Pedersen HE. The ossicles of the semilunar cartilages of rodents. Anat Rec 1949;105:1–9.
24. Gamer LW, Xiang L, Rosen V. Formation and maturation of the murine meniscus. J Orthop Res 2017;35:1683–9.
25. Mohankumar R, Palisch A, Khan W, White LM, Morrison WB. Meniscal ossicle: posttraumatic origin and association with posterior meniscal root tears. AJR Am J Roentgenol 2014;203:1040–6.
26. Ververidis AN, Keskinis A, Paraskevopoulos K, Ververidis NA, Tottas S, Drosos G, *et al*. Diagnostic and therapeutic approach to meniscal ossification: a systematic review. Knee Surg Sports Traumatol Arthrosc 2021;29:3037–48.
27. Verdelis K, Lukashova L, Atti E, Mayer-Kuckuk P, Peterson MG, Tetradis S, *et al*. MicroCT morphometry analysis of mouse cancellous bone: intra- and inter-system reproducibility. Bone 2011;49:580–7.
28. Bonnet N, Laroche N, Vico L, Dolleans E, Courteix D, Benhamou CL. Assessment of trabecular bone microarchitecture by two different x-ray microcomputed tomographs: a comparative study of the rat distal tibia using Skyscan and Scanco devices. Med Phys 2009;36:1286–97.
29. Steiner L, Synek A, Pahr DH. Comparison of different microCT-based morphology assessment tools using human trabecular bone. Bone Rep 2020;12, 100261.
30. Mys K, Varga P, Stockmans F, Gueorguiev B, Wyers CE, van den Bergh JPW, *et al*. Quantification of 3D microstructural parameters of trabecular bone is affected by the analysis software. Bone 2020;142, 115653.
31. Glasson SS, Blanchet TJ, Morris EA. The surgical destabilization of the medial meniscus (DMM) model of osteoarthritis in the 129/SvEv mouse. Osteoarthritis Cartilage 2007;15:1061–9.
32. Kadri A, Funck-Brentano T, Lin H, Ea HK, Hannouche D, Marty C, *et al*. Inhibition of bone resorption blunts osteoarthritis in mice with high bone remodelling. Ann Rheum Dis 2010;69:1533–8.
33. Nukuto K, Matsushita T, Kamada K, Nishida K, Nagai K, Kanzaki N, *et al*. Development and analysis of mouse medial meniscus posterior root tear model. Calcif Tissue Int 2023;112:55–65.
34. Camacho A, Simão M, Ea HK, Cohen-Solal M, Richette P, Branco J, *et al*. Iron overload in a murine model of hereditary hemochromatosis is associated with accelerated progression of osteoarthritis under mechanical stress. Osteoarthritis Cartilage 2016;24:494–502.
35. He YJ, Liang X, Zhang XX, Li SS, Sun Y, Li TF. PTH1-34 inhibited TNF-alpha expression and antagonized TNF-alpha-induced MMP13 expression in MIO mice. Int Immunopharmacol 2021;91, 107191.
36. Jia H, Ma X, Wei Y, Tong W, Tower RJ, Chandra A, *et al*. Loading-induced reduction in sclerostin as a mechanism of subchondral bone plate sclerosis in mouse knee joints during late-stage osteoarthritis. Arthritis Rheumatol 2018;70:230–41.
37. Rosch G, Muschter D, Taheri S, El Bagdadi K, Dorn C, Meurer A, *et al*. β2-Adrenoceptor deficiency results in increased calcified cartilage thickness and subchondral bone remodeling in murine experimental osteoarthritis. Front Immunol 2021;12, 801505.
38. Nielsen RH, Bay-Jensen AC, Byrjalsen I, Karsdal MA. Oral salmon calcitonin reduces cartilage and bone pathology in an osteoarthritis rat model with increased subchondral bone turnover. Osteoarthritis Cartilage 2011;19:466–73.
39. Yang G, Wang K, Song H, Zhu R, Ding S, Yang H, *et al*. Celastrol ameliorates osteoarthritis via regulating TLR2/NF-kappaB signaling pathway. Front Pharmacol 2022;13, 963506.
40. Burghardt AJ, Link TM, Majumdar S. High-resolution computed tomography for clinical imaging of bone microarchitecture. Clin Orthop Relat Res 2011;469:2179–93.
41. Bouxsein ML, Boyd SK, Christiansen BA, Guldberg RE, Jepsen KJ, Muller R. Guidelines for assessment of bone microstructure in rodents using micro-computed tomography. J Bone Miner Res 2010;25:1468–86.
42. Yi N, Mi Y, Xu X, Li N, Zeng F, Yan K, *et al*. Baicalein alleviates osteoarthritis progression in mice by protecting subchondral bone and suppressing chondrocyte apoptosis based on network pharmacology. Front Pharmacol 2021;12, 788392.
43. Chen S, Xu H, He Y, Meng C, Fan Y, Qu Y, *et al*. Carveol alleviates osteoarthritis progression by acting on synovial macrophage polarization transformation: an in vitro and in vivo study. Chem Biol Interact 2023;387, 110781.
44. Chen S, Meng C, He Y, Xu H, Qu Y, Wang Y, *et al*. An in vitro and in vivo study: valencene protects cartilage and alleviates the progression of osteoarthritis by anti-oxidative stress and anti-inflammatory effects. Int Immunopharmacol 2023;123, 110726.
45. Ma JJ, Ying J, Wang JY, Xu TT, Xia HT, Jin HT, *et al*. CD38 drives progress of osteoarthritis by affecting cartilage homeostasis. Orthop Surg 2022;14:946–54.
46. Lorenz J, Grassel S. Experimental osteoarthritis models in mice. Methods Mol Biol 2014;1194:401–19.
47. Herrero-Beaumont G, Roman-Blas JA, Bruyere O, Cooper C, Kanis J, Maggi S, *et al*. Clinical settings in knee osteoarthritis: pathophysiology guides treatment. Maturitas 2017;96:54–7.
48. Herrero-Beaumont G, Roman-Blas JA. Osteoarthritis: Osteoporotic OA: a reasonable target for bone-acting agents. Nat Rev Rheumatol 2013;9:448–50.
49. Roman-Blas JA, Herrero-Beaumont G. Targeting subchondral bone in osteoporotic osteoarthritis. Arthritis Res Ther 2014;16:494.
50. Burr DB, Gallant MA. Bone remodelling in osteoarthritis. Nat Rev Rheumatol 2012;8:665–73.
51. Chen MF, Hu CC, Hsu YH, Chiu YT, Chen KL, Ueng SWN, *et al*. Characterization and advancement of an evaluation method for the treatment of spontaneous osteoarthritis in STR/ort mice: GRGDS peptides as a potential treatment for osteoarthritis. Biomedicines 2023;11:1111.
52. Tu M, Yang M, Yu N, Zhen G, Wan M, Liu W, *et al*. Inhibition of cyclooxygenase-2 activity in subchondral bone modifies a subtype of osteoarthritis. Bone Res 2019;7:29.

53. Sanada Y, Ikuta Y, Ding C, Shinohara M, Yimiti D, Ishitobi H, *et al*. Senescence-accelerated mice prone 8 (SAMP8) in male as a spontaneous osteoarthritis model. Arthritis Res Ther 2022;24:235.
54. Nagira K, Ikuta Y, Shinohara M, Sanada Y, Omoto T, Kanaya H, *et al*. Histological scoring system for subchondral bone changes in murine models of joint aging and osteoarthritis. Sci Rep 2020;10, 10077.
55. Olah T, Cucchiarini M, Madry H. Subchondral bone remodeling patterns in larger animal models of meniscal injuries inducing knee osteoarthritis – a systematic review. Knee Surg Sports Traumatol Arthrosc 2023.
56. Herbst EC, Felder AA, Evans LAE, Ajami S, Javaheri B, Pitsillides AA. A new straightforward method for semi-automated segmentation of trabecular bone from cortical bone in diverse and challenging morphologies. R Soc Open Sci 2021;8, 210408.
57. Mahdi H, Hardisty M, Fullerton K, Vachhani K, Nam D, Whyne C. Open-source pipeline for automatic segmentation and microstructural analysis of murine knee subchondral bone. Bone 2023;167, 116616.
58. Jarraya M, Roemer FW, Englund M, Crema MD, Gale HI, Hayashi D, *et al*. Meniscus morphology: does tear type matter? A narrative review with focus on relevance for osteoarthritis research. Semin Arthritis Rheum 2017;46:552–61.
59. Ma HL, Blanchet TJ, Peluso D, Hopkins B, Morris EA, Glasson SS. Osteoarthritis severity is sex dependent in a surgical mouse model. Osteoarthritis Cartilage 2007;15:695–700.
60. Pucha KA, McKinney JM, Fuller JM, Willett NJ. Characterization of OA development between sexes in the rat medial meniscal transection model. Osteoarthr Cartil Open 2020;2, 100066.
61. Malfait AM, Little CB. On the predictive utility of animal models of osteoarthritis. Arthritis Res Ther 2015;17:225.
62. Hunter DJ, Little CB. The great debate: should osteoarthritis research focus on "mice" or "men"? Osteoarthritis Cartilage 2016;24:4–8.
63. Chan DD, Mashiatulla M, Li J, Ross RD, Pendyala M, Patwa A, *et al*. Contrast-enhanced micro-computed tomography of compartment and time-dependent changes in femoral cartilage and subchondral plate in a murine model of osteoarthritis. Anat Rec 2023;306:92–109.
64. Sun Q, Zhang Y, Ding Y, Xie W, Li H, Li S, *et al*. Inhibition of PGE2 in subchondral bone attenuates osteoarthritis. Cells 2022;11:2760.
65. Zaki S, Smith MM, Smith SM, Little CB. Differential patterns of pathology in and interaction between joint tissues in long-term osteoarthritis with different initiating causes: phenotype matters. Osteoarthritis Cartilage 2020;28:953–65.
66. Das Neves Borges P, Vincent TL, Marenzana M. Automated assessment of bone changes in cross-sectional micro-CT studies of murine experimental osteoarthritis. PLoS One 2017;12, e0174294.
67. Jackson MT, Moradi B, Zaki S, Smith MM, McCracken S, Smith SM, *et al*. Depletion of protease-activated receptor 2 but not protease-activated receptor 1 may confer protection against osteoarthritis in mice through extracartilaginous mechanisms. Arthritis Rheumatol 2014;66:3337–48.
68. Kung LHW, Ravi V, Rowley L, Angelucci C, Fosang AJ, Bell KM, *et al*. Cartilage MicroRNA dysregulation during the onset and progression of mouse osteoarthritis is independent of aggrecanolysis and overlaps with candidates from end-stage human disease. Arthritis Rheumatol 2018;70:383–95.
69. Kim GM, Kim J, Lee JY, Park MC, Lee SY. IgSF11 deficiency alleviates osteoarthritis in mice by suppressing early subchondral bone changes. Exp Mol Med 2023;55:2576–85.
70. Su W, Liu G, Liu X, Zhou Y, Sun Q, Zhen G, *et al*. Angiogenesis stimulated by elevated PDGF-BB in subchondral bone contributes to osteoarthritis development. JCI Insight 2020;5, e135446.
71. Sun Q, Zhen G, Li TP, Guo Q, Li Y, Su W, *et al*. Parathyroid hormone attenuates osteoarthritis pain by remodeling subchondral bone in mice. Elife 2021;10, e66532.
72. Huesa C, Ortiz AC, Dunning L, McGavin L, Bennett L, McIntosh K, *et al*. Proteinase-activated receptor 2 modulates OA-related pain, cartilage and bone pathology. Ann Rheum Dis 2016;75:1989–97.
73. Li W, Cai L, Zhang Y, Cui L, Shen G. Intra-articular resveratrol injection prevents osteoarthritis progression in a mouse model by activating SIRT1 and thereby silencing HIF-2alpha. J Orthop Res 2015;33:1061–70.
74. Stock M, Menges S, Eitzinger N, Gesslein M, Botschner R, Wormser L, *et al*. A dual role of upper zone of growth plate and cartilage matrix-associated protein in human and mouse osteoarthritic cartilage: inhibition of aggrecanases and promotion of bone turnover. Arthritis Rheumatol 2017;69:1233–45.
75. Okura T, Matsushita M, Mishima K, Esaki R, Seki T, Ishiguro N, *et al*. Activated FGFR3 prevents subchondral bone sclerosis during the development of osteoarthritis in transgenic mice with achondroplasia. J Orthop Res 2018;36:300–8.
76. Miller RE, Tran PB, Ishihara S, Larkin J, Malfait AM. Therapeutic effects of an anti-ADAMTS-5 antibody on joint damage and mechanical allodynia in a murine model of osteoarthritis. Osteoarthritis Cartilage 2016;24:299–306.
77. Xue T, Ning K, Yang B, Dou X, Liu S, Wang D, *et al*. Effects of immobilization and swimming on the progression of osteoarthritis in mice. Int J Mol Sci 2022;24:535.
78. Liu B, Ji C, Shao Y, Liang T, He J, Jiang H, *et al*. Etoricoxib decreases subchondral bone mass and attenuates biomechanical properties at the early stage of osteoarthritis in a mouse model. Biomed Pharmacother 2020;127, 110144.
79. Ji CC, Liu B, Shao YJ, Liang T, Jiang HY, Chen GD, *et al*. Microstructure and mechanical properties of subchondral bone are negatively regulated by tramadol in osteoarthritis in mice. Biosci Rep 2020;40. BSR20194207.
80. Holyoak DT, Chlebek C, Kim MJ, Wright TM, Otero M, van der Meulen MCH. Low-level cyclic tibial compression attenuates early osteoarthritis progression after joint injury in mice. Osteoarthritis Cartilage 2019;27:1526–36.
81. Shin Y, Cho D, Kim SK, Chun JS. STING mediates experimental osteoarthritis and mechanical allodynia in mouse. Arthritis Res Ther 2023;25:90.
82. Uchimura T, Foote AT, Smith EL, Matzkin EG, Zeng L. Insulin-like growth factor II (IGF-II) inhibits IL-1beta-induced cartilage matrix loss and promotes cartilage integrity in experimental osteoarthritis. J Cell Biochem 2015;116:2858–69.
83. Corciulo C, Scheffler JM, Humeniuk P, Del Carpio Pons A, Stubelius A, Von Mentzer U, *et al*. Physiological levels of estradiol limit murine osteoarthritis progression. J Endocrinol 2022;255:39–51.
84. Botter SM, Glasson SS, Hopkins B, Clockaerts S, Weinans H, van Leeuwen JP, *et al*. ADAMTS5-/- mice have less subchondral bone changes after induction of osteoarthritis through surgical instability: implications for a link between cartilage and subchondral bone changes. Osteoarthritis Cartilage 2009;17:636–45.
85. Waung JA, Maynard SA, Gopal S, Gogakos A, Logan JG, Williams GR, *et al*. Quantitative X-ray microradiography for high-throughput phenotyping of osteoarthritis in mice. Osteoarthritis Cartilage 2014;22:1396–400.
86. Thysen S, Luyten FP, Lories RJ. Loss of Frzb and Sfrp1 differentially affects joint homeostasis in instability-induced osteoarthritis. Osteoarthritis Cartilage 2015;23:275–9.
87. Moodie JP, Stok KS, Muller R, Vincent TL, Shefelbine SJ. Multimodal imaging demonstrates concomitant changes in bone and cartilage after destabilisation of the medial meniscus and increased joint laxity. Osteoarthritis Cartilage 2011;19:163–70.

88. Valverde-Franco G, Pelletier JP, Fahmi H, Hum D, Matsuo K, Lussier B, *et al*. In vivo bone-specific EphB4 overexpression in mice protects both subchondral bone and cartilage during osteoarthritis. Arthritis Rheum 2012;64:3614–25.
89. Jin J, Yu X, Hu Z, Tang S, Zhong X, Xu J, *et al*. Isofraxidin targets the TLR4/MD-2 axis to prevent osteoarthritis development. Food Funct 2018;9:5641–52.
90. Shin SY, Pozzi A, Boyd SK, Clark AL. Integrin α1β1 protects against signs of post-traumatic osteoarthritis in the female murine knee partially via regulation of epidermal growth factor receptor signalling. Osteoarthritis Cartilage 2016;24:1795–806.
91. Zheng W, Tao Z, Chen C, Zhang C, Zhang H, Ying X, *et al*. Plumbagin prevents IL-1beta-induced inflammatory response in human osteoarthritis chondrocytes and prevents the progression of osteoarthritis in mice. Inflammation 2017;40:849–60.
92. Huang H, Skelly JD, Ayers DC, Song J. Age-dependent changes in the articular cartilage and subchondral bone of C57BL/6 mice after surgical destabilization of medial meniscus. Sci Rep 2017;7, 42294.
93. Mevel E, Shutter JA, Ding X, Mattingly BT, Williams JN, Li Y, *et al*. Systemic inhibition or global deletion of CaMKK2 protects against post-traumatic osteoarthritis. Osteoarthritis Cartilage 2022;30:124–36.
94. Zhang L, Kirkwood CL, Sohn J, Lau A, Bayers-Thering M, Bali SK, *et al*. Expansion of myeloid-derived suppressor cells contributes to metabolic osteoarthritis through subchondral bone remodeling. Arthritis Res Ther 2021;23:287.
95. Tornqvist AE, Grahnemo L, Nilsson KH, Funck-Brentano T, Ohlsson C, Moverare-Skrtic S. Wnt16 overexpression in osteoblasts increases the subchondral bone mass but has no impact on osteoarthritis in young adult female mice. Calcif Tissue Int 2020;107:31–40.
96. Renaudin F, Oudina K, Gerbaix M, McGilligan Subilia M, Paccaud J, Jaquet V, *et al*. NADPH oxidase 4 deficiency attenuates experimental osteoarthritis in mice. RMD Open 2023;9, e002856.
97. Staines KA, Ikpegbu E, Tornqvist AE, Dillon S, Javaheri B, Amin AK, *et al*. Conditional deletion of E11/podoplanin in bone protects against load-induced osteoarthritis. BMC Musculoskelet Disord 2019;20:344.
98. Pan J, Wang B, Li W, Zhou X, Scherr T, Yang Y, *et al*. Elevated cross-talk between subchondral bone and cartilage in osteoarthritic joints. Bone 2012;51:212–7.
99. Li Q, Han B, Wang C, Tong W, Wei Y, Tseng WJ, *et al*. Mediation of cartilage matrix degeneration and fibrillation by decorin in post-traumatic osteoarthritis. Arthritis Rheumatol 2020;72:1266–77.
100. Han B, Li Q, Wang C, Chandrasekaran P, Zhou Y, Qin L, *et al*. Differentiated activities of decorin and biglycan in the progression of post-traumatic osteoarthritis. Osteoarthritis Cartilage 2021;29:1181–92.
101. Samvelyan HJ, Huesa C, Cui L, Farquharson C, Staines KA. The role of accelerated growth plate fusion in the absence of SOCS2 on osteoarthritis vulnerability. Bone Joint Res 2022;11:162–70.
102. Tornqvist AE, Sophocleous A, Ralston SH, Ohlsson C, Svensson J. Liver-derived IGF-I is not required for protection against osteoarthritis in male mice. Am J Physiol Endocrinol Metab 2019;317:E1150–7.
103. Gil Alabarse P, Chen LY, Oliveira P, Qin H, Liu-Bryan R. Targeting CD38 to suppress osteoarthritis development and associated pain after joint injury in mice. Arthritis Rheumatol 2023;75:364–74.
104. Hu X, Ji X, Yang M, Fan S, Wang J, Lu M, *et al*. Cdc42 is essential for both articular cartilage degeneration and subchondral bone deterioration in experimental osteoarthritis. J Bone Miner Res 2018;33:945–58.
105. Wei Y, Luo L, Gui T, Yu F, Yan L, Yao L, *et al*. Targeting cartilage EGFR pathway for osteoarthritis treatment. Sci Transl Med 2021;13, eabb3946.
106. Reece DS, Thote T, Lin ASP, Willett NJ, Guldberg RE. Contrast enhanced μCT imaging of early articular changes in a preclinical model of osteoarthritis. Osteoarthritis Cartilage 2018;26:118–27.
107. Yu DG, Nie SB, Liu FX, Wu CL, Tian B, Wang WG, *et al*. Dynamic alterations in microarchitecture, mineralization and mechanical property of subchondral bone in rat medial meniscal tear model of osteoarthritis. Chin Med J 2015;128:2879–86.
108. Aso K, Shahtaheri SM, Hill R, Wilson D, McWilliams DF, Nwosu LN, *et al*. Contribution of nerves within osteochondral channels to osteoarthritis knee pain in humans and rats. Osteoarthritis Cartilage 2020;28:1245–54.
109. Lin ASP, Reece DS, Thote T, Sridaran S, Stevens HY, Willett NJ, *et al*. Intra-articular delivery of micronized dehydrated human amnion/chorion membrane reduces degenerative changes after onset of post-traumatic osteoarthritis. Front Bioeng Biotechnol 2023;11, 1224141.
110. Bagi CM, Berryman ER, Teo S, Lane NE. Oral administration of undenatured native chicken type II collagen (UC-II) diminished deterioration of articular cartilage in a rat model of osteoarthritis (OA). Osteoarthritis Cartilage 2017;25:2080–90.
111. Bagi CM, Berryman E, Zakur DE, Wilkie D, Andresen CJ. Effect of antiresorptive and anabolic bone therapy on development of osteoarthritis in a posttraumatic rat model of OA. Arthritis Res Ther 2015;17:315.
112. Bagi CM, Zakur DE, Berryman E, Andresen CJ, Wilkie D. Correlation between muCT imaging, histology and functional capacity of the osteoarthritic knee in the rat model of osteoarthritis. J Transl Med 2015;13:276.
113. Iijima H, Aoyama T, Ito A, Yamaguchi S, Nagai M, Tajino J, *et al*. Effects of short-term gentle treadmill walking on subchondral bone in a rat model of instability-induced osteoarthritis. Osteoarthritis Cartilage 2015;23:1563–74.
114. Iijima H, Aoyama T, Tajino J, Ito A, Nagai M, Yamaguchi S, *et al*. Subchondral plate porosity colocalizes with the point of mechanical load during ambulation in a rat knee model of post-traumatic osteoarthritis. Osteoarthritis Cartilage 2016;24:354–63.
115. Iijima H, Ito A, Nagai M, Tajino J, Yamaguchi S, Kiyan W, *et al*. Physiological exercise loading suppresses post-traumatic osteoarthritis progression via an increase in bone morphogenetic proteins expression in an experimental rat knee model. Osteoarthritis Cartilage 2017;25:964–75.
116. Iijima H, Aoyama T, Ito A, Tajino J, Yamaguchi S, Nagai M, *et al*. Exercise intervention increases expression of bone morphogenetic proteins and prevents the progression of cartilage-subchondral bone lesions in a post-traumatic rat knee model. Osteoarthritis Cartilage 2016;24:1092–102.
117. Fang H, Huang L, Welch I, Norley C, Holdsworth DW, Beier F, *et al*. Early changes of articular cartilage and subchondral bone in the DMM mouse model of osteoarthritis. Sci Rep 2018;8:2855.
118. Wang TR, Wang HD, Chen W, Yu TB, Qin Y, Zhang YZ. Proximal fibular osteotomy alleviates medial compartment knee osteoarthritis in a mouse model. Int Orthop 2020;44:1107–13.
119. Yan J, Feng G, Yang Y, Ding D, Ma L, Zhao X, *et al*. Autophagy attenuates osteoarthritis in mice by inhibiting chondrocyte pyroptosis and improving subchondral bone remodeling. Biomol Biomed 2023;23:77–88.
120. Meng Z, Xin L, Fan B. SDF-1alpha promotes subchondral bone sclerosis and aggravates osteoarthritis by regulating the proliferation and osteogenic differentiation of bone marrow mesenchymal stem cells. BMC Musculoskelet Disord 2023;24:275.
121. Lin C, Shao Y, Zeng C, Zhao C, Fang H, Wang L, *et al*. Blocking PI3K/AKT signaling inhibits bone sclerosis in subchondral bone and attenuates post-traumatic osteoarthritis. J Cell Physiol 2018;233:6135–47.

122. Shao YJ, Chen X, Chen Z, Jiang HY, Zhong DY, Wang YF, *et al*. Sensory nerves protect from the progression of early stage osteoarthritis in mice. Connect Tissue Res 2020;61:445–55.
123. Arakawa K, Takahata K, Enomoto S, Oka Y, Ozone K, Nakagaki S, *et al*. The difference in joint instability affects the onset of cartilage degeneration or subchondral bone changes. Osteoarthritis Cartilage 2022;30:451–60.
124. Chen L, Ni Z, Huang J, Zhang R, Zhang J, Zhang B, *et al*. Long term usage of dexamethasone accelerating accelerates the initiation of osteoarthritis via enhancing chondrocyte apoptosis and the extracellular matrix calcification and apoptosis of chondrocytes. Int J Biol Sci 2021;17:4140–53.
125. Lorenz J, Seebach E, Hackmayer G, Greth C, Bauer RJ, Kleinschmidt K, *et al*. Melanocortin 1 receptor-signaling deficiency results in an articular cartilage phenotype and accelerates pathogenesis of surgically induced murine osteoarthritis. PLoS One 2014;9, e105858.
126. Guo H, Ding D, Wang L, Yan J, Ma L, Jin Q. Metformin attenuates osteoclast-mediated abnormal subchondral bone remodeling and alleviates osteoarthritis via AMPK/NF-kappaB/ERK signaling pathway. PLoS One 2021;16, e0261127.
127. Yan J, Ding D, Feng G, Yang Y, Zhou Y, Ma L, *et al*. Metformin reduces chondrocyte pyroptosis in an osteoarthritis mouse model by inhibiting NLRP3 inflammasome activation. Exp Ther Med 2022;23:222.
128. Huesa C, Dunning L, MacDougall K, Fegen M, Ortiz A, McCulloch K, *et al*. Moderate exercise protects against joint disease in a murine model of osteoarthritis. Front Physiol 2022;13, 1065278.
129. Amiable N, Martel-Pelletier J, Lussier B, Kwan Tat S, Pelletier JP, Boileau C. Proteinase-activated receptor-2 gene disruption limits the effect of osteoarthritis on cartilage in mice: a novel target in joint degradation. J Rheumatol 2011;38:911–20.
130. Li G, Liu S, Chen Y, Xu H, Qi T, Xiong A, *et al*. Teriparatide ameliorates articular cartilage degradation and aberrant subchondral bone remodeling in DMM mice. J Orthop Translat 2023;38:241–55.
131. Wang H, Zhang C, Zhu S, Gao C, Gao Q, Huang R, *et al*. Low-frequency whole-body vibration can enhance cartilage degradation with slight changes in subchondral bone in mice with knee osteoarthritis and does not have any morphologic effect on normal joints. PLoS One 2023;18, e0270074.
132. Sambamurthy N, Nguyen V, Smalley R, Xiao R, Hankenson K, Gan J, *et al*. Chemokine receptor-7 (CCR7) deficiency leads to delayed development of joint damage and functional deficits in a murine model of osteoarthritis. J Orthop Res 2018;36:864–75.
133. Sambamurthy N, Zhou C, Nguyen V, Smalley R, Hankenson KD, Dodge GR, *et al*. Deficiency of the pattern-recognition receptor CD14 protects against joint pathology and functional decline in a murine model of osteoarthritis. PLoS One 2018;13, e0206217.
134. Collins JA, Kim CJ, Coleman A, Little A, Perez MM, Clarke EJ, *et al*. Cartilage-specific Sirt6 deficiency represses IGF-1 and enhances osteoarthritis severity in mice. Ann Rheum Dis 2023;82:1464–73.
135. Zhou S, Wang Z, Tang J, Li W, Huang J, Xu W, *et al*. Exogenous fibroblast growth factor 9 attenuates cartilage degradation and aggravates osteophyte formation in post-traumatic osteoarthritis. Osteoarthritis Cartilage 2016;24:2181–92.
136. Ouhaddi Y, Nebbaki SS, Habouri L, Afif H, Lussier B, Kapoor M, *et al*. Exacerbation of aging-associated and instability-induced murine osteoarthritis with deletion of D prostanoid receptor 1, a prostaglandin D2 receptor. Arthritis Rheumatol 2017;69:1784–95.
137. Liang S, Lv ZT, Zhang JM, Wang YT, Dong YH, Wang ZG, *et al*. Necrostatin-1 attenuates trauma-induced mouse osteoarthritis and IL-1beta induced apoptosis via HMGB1/TLR4/SDF-1 in primary mouse chondrocytes. Front Pharmacol 2018;9:1378.
138. Hu J, Zhou J, Wu J, Chen Q, Du W, Fu F, *et al*. Loganin ameliorates cartilage degeneration and osteoarthritis development in an osteoarthritis mouse model through inhibition of NF-κB activity and pyroptosis in chondrocytes. J Ethnopharmacol 2020;247, 112261.
139. Najar M, Ouhaddi Y, Pare F, Lussier B, Urade Y, Kapoor M, *et al*. Role of lipocalin-type prostaglandin D synthase in experimental osteoarthritis. Arthritis Rheumatol 2020;72:1524–33.
140. Muttigi MS, Kim BJ, Choi B, Han I, Park H, Lee SH. Matrilin-3-primed adipose-derived mesenchymal stromal cell spheroids prevent mesenchymal stromal-cell-derived chondrocyte hypertrophy. Int J Mol Sci 2020;21:8911.
141. Ling H, Zeng Q, Ge Q, Chen J, Yuan W, Xu R, *et al*. Osteoking decelerates cartilage degeneration in DMM-induced osteoarthritic mice model through TGF-beta/smad-dependent manner. Front Pharmacol 2021;12, 678810.
142. Yan J, Feng G, Ma L, Chen Z, Jin Q. Metformin alleviates osteoarthritis in mice by inhibiting chondrocyte ferroptosis and improving subchondral osteosclerosis and angiogenesis. J Orthop Surg Res 2022;17:333.
143. Huang H, Veien ES, Zhang H, Ayers DC, Song J. Skeletal characterization of Smurf2-deficient mice and in vitro analysis of Smurf2-deficient chondrocytes. PLoS One 2016;11, e0148088.
144. Doyran B, Tong W, Li Q, Jia H, Zhang X, Chen C, *et al*. Nanoindentation modulus of murine cartilage: a sensitive indicator of the initiation and progression of post-traumatic osteoarthritis. Osteoarthritis Cartilage 2017;25:108–17.
145. Tao T, Luo D, Gao C, Liu H, Lei Z, Liu W, *et al*. Src homology 2 domain-containing protein tyrosine phosphatase promotes inflammation and accelerates osteoarthritis by activating beta-catenin. Front Cell Dev Biol 2021;9, 646386.
146. Samvelyan HJ, Madi K, Tornqvist AE, Javaheri B, Staines KA. Characterisation of growth plate dynamics in murine models of osteoarthritis. Front Endocrinol 2021;12, 734988.
147. Clement-Lacroix P, Little CB, Smith MM, Cottereaux C, Merciris D, Meurisse S, *et al*. Pharmacological characterization of GLPG1972/S201086, a potent and selective small-molecule inhibitor of ADAMTS5. Osteoarthritis Cartilage 2022;30:291–301.
148. Ye W, Guo H, Yang X, Yang L, He C. Pulsed electromagnetic field versus whole body vibration on cartilage and subchondral trabecular bone in mice with knee osteoarthritis. Bioelectromagnetics 2020;41:298–307.
149. Moritake A, Kawao N, Okada K, Tatsumi K, Ishida M, Okumoto K, *et al*. Plasminogen activator inhibitor-1 deficiency enhances subchondral osteopenia after induction of osteoarthritis in mice. BMC Musculoskelet Disord 2017;18:392.
150. Wang K, Lu X, Li X, Zhang Y, Xu R, Lou Y, *et al*. Dual protective role of velutin against articular cartilage degeneration and subchondral bone loss via the p38 signaling pathway in murine osteoarthritis. Front Endocrinol 2022;13, 926934.
151. Gao P, Rao ZW, Li M, Sun XY, Gao QY, Shang TZ, *et al*. Tetrandrine represses inflammation and attenuates osteoarthritis by selective inhibition of COX-2. Curr Med Sci 2023;43:505–13.
152. Park E, Lee CG, Han SJ, Yun SH, Hwang S, Jeon H, *et al*. Antiosteoarthritic effect of morroniside in chondrocyte inflammation and destabilization of medial meniscus-induced mouse model. Int J Mol Sci 2021;22:2987.
153. Oliviero S, Millard E, Chen Z, Rayson A, Roberts BC, Ismail HMS, *et al*. Accuracy of in vivo microCT imaging in assessing the microstructural properties of the mouse tibia subchondral bone. Front Endocrinol 2022;13, 1016321.

154. Wang P, Xu J, Sun Q, Ge Q, Qiu M, Zou K, *et al*. Chondroprotective mechanism of *Eucommia ulmoides* Oliv.-*Glycyrrhiza uralensis* Fisch. couplet medicines in knee osteoarthritis via experimental study and network pharmacology analysis. Drug Des Devel Ther 2023;17:633–46.
155. Soki FN, Yoshida R, Paglia DN, Duong LT, Hansen MF, Drissi H. Articular cartilage protection in Ctsk(-/-) mice is associated with cellular and molecular changes in subchondral bone and cartilage matrix. J Cell Physiol 2018;233:8666–76.
156. Au M, Liu Z, Rong L, Zheng Y, Wen C. Endothelin-1 induces chondrocyte senescence and cartilage damage via endothelin receptor type B in a post-traumatic osteoarthritis mouse model. Osteoarthritis Cartilage 2020;28:1559–71.
157. Yu DG, Yu B, Mao YQ, Zhao X, Wang XQ, Ding HF, *et al*. Efficacy of zoledronic acid in treatment of teoarthritis is dependent on the disease progression stage in rat medial meniscal tear model. Acta Pharmacol Sin 2012;33:924–34.
158. Yu DG, Ding HF, Mao YQ, Liu M, Yu B, Zhao X, *et al*. Strontium ranelate reduces cartilage degeneration and subchondral bone remodeling in rat osteoarthritis model. Acta Pharmacol Sin 2013;34:393–402.
159. Morita Y, Ito H, Ishikawa M, Fujii T, Furu M, Azukizawa M, *et al*. Subchondral bone fragility with meniscal tear accelerates and parathyroid hormone decelerates articular cartilage degeneration in rat osteoarthritis model. J Orthop Res 2018;36:1959–68.
160. Kloefkorn HE, Allen KD. Quantitative histological grading methods to assess subchondral bone and synovium changes subsequent to medial meniscus transection in the rat. Connect Tissue Res 2017;58:373–85.
161. Tsai LC, Cooper ES, Hetzendorfer KM, Warren GL, Chang YH, Willett NJ. Effects of treadmill running and limb immobilization on knee cartilage degeneration and locomotor joint kinematics in rats following knee meniscal transection. Osteoarthritis Cartilage 2019;27:1851–9.
162. Liang G, Zhao J, Zhao D, Dou Y, Huang H, Yang W, *et al*. Longbie capsules reduce bone loss in the subchondral bone of rats with comorbid osteoporosis and osteoarthritis by regulating metabolite alterations. Front Med 2023;10, 1256238.
163. Ding D, Wang L, Yan J, Zhou Y, Feng G, Ma L, *et al*. Zoledronic acid generates a spatiotemporal effect to attenuate osteoarthritis by inhibiting potential Wnt5a-associated abnormal subchondral bone resorption. PLoS One 2022;17, e0271485.
164. Ding D, Yan J, Feng G, Zhou Y, Ma L, Jin Q. Dihydroartemisinin attenuates osteoclast formation and bone resorption via inhibiting the NFkappaB, MAPK and NFATc1 signaling pathways and alleviates osteoarthritis. Int J Mol Med 2022;49:4.
165. Hu W, Yao X, Li Y, Li J, Zhang J, Zou Z, *et al*. Injectable hydrogel with selenium nanoparticles delivery for sustained glutathione peroxidase activation and enhanced osteoarthritis therapeutics. Mater Today Bio 2023;23, 100864.